Published in final edited form as:
Dev Neurobiol. 2008 February 15; 68(3): 392–408. doi:10.1002/dneu.20596.

Inhibition of Müller Glial Cell Division Blocks Regeneration of the Light-Damaged Zebrafish Retina

Ryan Thummel, **Sean C. Kassen**, **Jacob E. Montgomery**, **Jennifer M. Enright**, and **David R. Hyde**
Department of Biological Sciences and the Center for Zebrafish Research, University of Notre Dame, Notre Dame, Indiana 46556

Abstract

The adult zebrafish retina possesses a robust regenerative response. In the light-damaged retina, Müller glial cell divisions precede regeneration of rod and cone photoreceptors. Neuronal progenitors, which arise from the Müller glia, continue to divide and use the Müller glial cell processes to migrate to the outer nuclear layer and replace the lost photoreceptors. We tested the necessity of Müller glial cell division for photoreceptor regeneration. As knockdown tools were unavailable for use in the adult zebrafish retina, we developed a method to conditionally inhibit the expression of specific proteins by *in vivo* electroporation of morpholinos. We determined that two separate morpholinos targeted against the proliferating cell nuclear antigen (PCNA) mRNA reduced PCNA protein levels. Furthermore, injection and *in vivo* electroporation of PCNA morpholinos immediately prior to starting intense light exposure inhibited both Müller glial cell proliferation and neuronal progenitor marker Pax6 expression. PCNA knockdown additionally resulted in decreased expression of glutamine synthetase in Müller glia and Müller glial cell death, while amacrine and ganglion cells were unaffected. Finally, histological and immunological methods showed that long-term effects of PCNA knockdown resulted in decreased numbers of Müller glia and the failure to regenerate rod photoreceptors, short single cones, and long single cones. These data suggest that Müller glial cell division is necessary for proper photoreceptor regeneration in the light-damaged zebrafish retina and are consistent with the Müller glia serving as the source of neuronal progenitor cells in regenerating teleost retinas.

Keywords

retinal regeneration; Müller glia; zebrafish; morpholino electroporation; stem cell

INTRODUCTION

Teleost fish exhibit persistent retinal neurogenesis throughout their lifetime. New retinal neurons originate from two stem cell populations: (1) the circumferential germinal zone (CGZ) (Johns and Easter, 1977; Hagedorn and Fernald, 1992; Marcus et al., 1999), which is located at the retinal margin and is the source of all adult retinal cell types except for rod photoreceptors and (2) adult stem cells scattered across the inner nuclear layer (INL), which are the source for new rod photoreceptors (Straznicky and Gaze, 1971; Johns and Easter, 1977; Fischer and Reh, 2001; Wu et al., 2001).

Correspondence to: D.R. Hyde (dhyde@nd.edu).

This article contains supplementary material available via the Internet at http://www.mrw.interscience.wiley.com/suppmat/1932-8451/suppmat/

The cellular and molecular basis of retinal regeneration in adult teleost fish has been studied using protocols that cause the loss of one or more of the retinal cell types, including retinal puncture, chemical ablation, concentrated high temperature, and intense light treatment (Wolburg, 1975; Vihtelic and Hyde, 2000; Wu et al., 2001; Hitchcock et al., 2004; Yurco and Cameron, 2005; Fausett and Goldman, 2006; Raymond et al., 2006). We extensively characterized the regeneration response in zebrafish following two methods of damage: constant intense light treatment and intraocular injection of ouabain (Vihtelic and Hyde, 2000; Vihtelic et al., 2006; Fimbel et al., 2007). Intense light treatment specifically damages the photoreceptors of the retina (Vihtelic and Hyde, 2000; Vihtelic et al., 2006). In contrast, the intravitreal injection of a low concentration of ouabain specifically targets inner retinal neurons, with minimal damage to the photoreceptors (Wolburg, 1975; Fimbel et al., 2007). Both of these models revealed the Müller glia reenter the cell cycle and associate with the actively dividing neuronal progenitors (Vihtelic and Hyde, 2000; Vihtelic et al., 2006; Fimbel et al., 2007). Similarly, heat lesion and retinal puncture models demonstrated that the Müller glial cells actively divide and are the source of Pax6-expressing neuronal progenitors during retinal regeneration (Yurco and Cameron, 2005; Fausett and Goldman, 2006; Raymond et al., 2006). Thus, data from multiple damage models indicate the Müller glia reenter the cell cycle following retinal damage and may represent the primary source of neuronal progenitors during zebrafish retinal regeneration.

To examine the importance of Müller glial cell division during retinal regeneration, we developed a technique to electroporate morpholinos into the retina to knockdown proliferating cell nuclear antigen (PCNA) expression during light treatment. This procedure effectively blocked PCNA expression, and therefore cell division, in the light-damaged retina and resulted in a reduction in glutamine synthetase expression and the appearance of TUNEL-positive Müller glia. Furthermore, 28 days after terminating the constant light treatment, PCNA knockdown caused a persistent loss of Müller glial cells, rod photoreceptors, short single cones, and long single cone photoreceptors, based on immunological and histological analysis. These results suggest that inhibiting Müller glial cell division during the retinal regeneration response results in Müller cell apoptosis and a failure to regenerate photoreceptors. These results are consistent with the Müller glia, and not an independent cell population, serving as the initial ‘‘stem cell’’ source of the regenerating photoreceptors.

METHODS

Fish Maintenance

Wild-type AB and *albino* mutant zebrafish were maintained in the Center for Zebrafish Research in the AALAC-accredited Freimann Life Science Center at the University of Notre Dame. Facility lighting exposes the fish to an average light intensity (250 lux) under a 14 h: 10 h light:dark cycle at 28.5°C (Westerfield, 1995; Detrich et al., 1999). Adult fish were fed brine shrimp and flake food three times daily. For micro-injection studies, embryos were collected on the morning of the mating, immediately (0–15 min) after fertilization. All experimental protocols were approved by the animal use committee at the University of Notre Dame and were in compliance with the ARVO statement for the use of animals in vision research.

Microinjection of Morpholinos into Zebrafish Embryos

This study utilized five lissamine-tagged morpholinos: the Gene Tools (Philomath, OR) Standard Control morpholino (**5′-CCTCTTACCTCAGTTACAATTTATA-3′**), which has no complementary sequence in the zebrafish genome; two morpholinos targeted against PCNA, *pcna* MO1 (5′-**TGAACCAGACGTGCCTCAAACATTG-3′**) and *pcna* **MO2 (5′-**

TTTCTTAGTTTGGAGTAGGAGGAAC-3′); and two control morpholinos that contain 5 mismatched bases relative to the *pcna* experimental morpholinos, 5bmm **MO1 (5′-TGAAGCACACGTCCCTGAAAGATTG-3′)** and 5bmm MO2 (**5′-TTTGTTACTTTGGACTAGCAGCAAC-3′**). Morpholinos were resuspended in water to a concentration of 3 m*M* then diluted into working concentrations (0.5–1 m*M*) in either water or 1X Danieau Media (58 m*M* NaCl, 0.7 m*M* KCl, 0.4 m*M* $MgSO_4$, 0.6 m*M* $Ca(NO_3)_2$, and 5.0 m*M* HEPES, pH 7.6). Micro-injection of morpholinos into 1–4 cell stage embryos was performed as previously described (Nasevicius and Ekker, 2000; Thummel et al., 2004; Wei et al., 2004).

Immunoblot Analysis of Morpholino-Mediated Knockdown of PCNA

Protein isolation and immunoblot analysis was performed as previously described (Vihtelic et al., 1999; Shi et al., 2005). For these studies, total protein was isolated from either uninjected control and morpholino-injected embryos at 3 and 48-h post fertilization (hpf), or from uninjected control adult retinas. Total protein equivalent of either 1 embryo or 1/5th of a retina was combined with 4× sample buffer and 10× reducing buffer (Invitrogen, Carlsbad, CA). The sample was incubated at 70°C for 10 min and loaded onto a 4–12% SDS-PAGE (Invitrogen). The sample was electrophoresed and then transferred to a PVDF membrane (Amersham, Piscataway, NJ). The blot was blocked in PBS/5% nonfat dry milk/0.1% Tween-20 and then incubated with either an anti-PCNA monoclonal antibody (diluted 1:5000, Invitrogen) or an anti-β-actin monoclonal antibody (diluted 1:10,000, Calbiochem, San Diego, CA) overnight at 4°C in blocking buffer. The membrane was washed in PBS/0.1% Tween-20, and then incubated with an anti-mouse HRP-conjugated secondary antibody (diluted 1:10,000, Amersham). The ECL-Plus system (Amersham) was used to detect the secondary antibody as described (Vihtelic et al., 1999).

Constant Intense Light Treatment Protocol

Light treatment was performed as previously described (Vihtelic and Hyde, 2000; Vihtelic et al., 2006; Kassen et al., 2007). Prior to light treatment, 6–9-month-old *albino* zebrafish were maintained in constant darkness for 14 days. Fish were transferred to 1 or 2 L clear polycarbonate tanks and placed between four 150 W halogen lamps generating 3,500 lux light intensity at a water temperature of ~33°C. Fish underwent 1, 2, or 3 days of constant light treatment. Control and experimental groups were always treated simultaneously. For the long-term regeneration analysis, fish were exposed to 4 days of constant intense light, and returned to standard 14-h light: 10-h dark conditions for 28 days.

Injection and Electroporation of Morpholinos in Adult Zebrafish Retinas

Morpholino injection and electroporation was performed immediately prior to starting the light treatment. Dark-treated adult *albino* zebrafish were anesthetized in 2-phenoxyethanol and the outer most component of the cornea was removed with small forceps by grabbing the cornea near the ventral fissure and pulling across the eye. An incision was made in the cornea adjacent to the iris using a sapphire blade scalpel. A Hamilton syringe was used to inject 0.5 μL of 3.0 m*M* morpholino solution into the vitreous of the left eye, while the right eyes were not injected. Fish were revived following injection. After injecting 8–12 fish (~5 min), fish were individually reanesthetized for the electroporation event and transferred to a Petri dish filled with anesthesia. The fish was secured right-side down using a damp paper towel, leaving the left eye exposed and facing up. A 3-mm diameter platinum plate electrode (CUY 650-P3 Tweezers, Protech International) was used to direct the morpholino (which has a slightly positive charge due to the lissamine tag) into the dorsal half of the retina. Specifically, the positive electrode was used to gently press down on the eye near the ventral fissure. This caused the eye to rotate in the socket slightly, exposing the dorsal half of the

eye. The negative electrode was placed adjacent to the exposed dorsal half of the eye, taking care not to touch the electrode to the eye. Electroporation of the left eye was performed using a CUY21 Square Wave Electroporator (Protech International, San Antonio, TX). On the basis of the parameters used in the neonatal mouse (Matsuda and Cepko, 2004), 2 consecutive 50-ms pulses at 75 V with a 1-s pause between pulses were used. The electrodes were gently wiped with damp Kimwipes (Kimberly-Clark Professional, Roswell, GA) following each electroporation. The fish were then revived and placed directly into the light treatment.

Immunolabeling and Confocal Imaging

Following various lengths of time in the constant light treatment, fish were euthanized by anesthetic overdose and eyes were harvested and fixed overnight at 4°C in either 4% para-formaldehyde (in 5% sucrose/1X PBS) or 9:1 ethanolic formaldehyde (95% ethanol:37% formaldehyde). Following fixation, the eyes were washed in 5% sucrose/1X PBS three times for 20 min at room temperature, then cryoprotected by incubating in 30% sucrose overnight at 4°C. Eyes were washed in a 1:1 solution of 30% sucrose/Tissue Freezing Medium (TBS, Triangle Biomedical Sciences, Durham, NC) for 4 h at room temperature, then in a 1:2 dilution of 30% sucrose/TBS overnight. Eyes were finally embedded in 100% TBS and sectioned at 14 μm. The frozen sections were dried for 2 h at 50°C, followed by rehydration in 1X PBS.

Retinal sections were incubated in blocking solution (1X PBS/2% normal goat serum/1% DMSO/0.2% Triton-X 100) for 1 h at room temperature and then in blocking solution containing the primary antibody overnight at 4°C. The primary antibodies used for these studies were mouse monoclonal anti-PCNA antibody (1:1000, clone PC10, Sigma Chemical, St. Louis, MO), rabbit polyclonal anti-rhodopsin (1:5000, Vihtelic et al., 1999), rabbit polyclonal anti-UV opsin (1:1000, Vihtelic et al., 1999), rabbit polyclonal anti-green opsin (1:500, Vihtelic et al., 1999), rabbit polyclonal anti-blue opsin (1:250, Vihtelic et al., 1999), rabbit polyclonal anti-Pax6 (1:100, Covance, Berkeley, CA), rabbit polyclonal anti-H3P (1:100, Upstate, Billerica, MA), mouse monoclonal anti-HuC/D antibody (1:100, Molecular Probes, Carlsbad, CA), rabbit polyclonal anti-GFAP antibody (1:500, DAKO, Denmark) and mouse monoclonal anti-glutamine synthetase antibody (1:500, Chemicon International, Temecula, CA). The sections were washed in 1X PBS/0.05% Tween-20 and incubated for 1 h at room temperature in a 1:500 dilution of an Alexa Fluor 488, 594, or 647 goat anti-primary secondary antibody (Molecular Probes) diluted in 1X PBS/0.05% Tween-20. Nuclei were labeled with TO-PRO-3 (Molecular Probes). Sections were washed in 1X PBS/0.05% Tween-20, 1X PBS, and cover-mounted using ProLong Gold (Molecular Probes).

For Pax6 immunolocalization, an antigen retrieval protocol was used. Eyes were processed, embedded, and sectioned as described above. Following rehydration, slides were incubated in preheated 1× AntigenPlus buffer pH 10 (Novagen, Madison, WI) for 25 min at 95°C. Slides were allowed to cool for 45 min and immunolabeled as described above.

Confocal microscopy was performed with a 1024 Bio-Rad confocal microscope on retinal sections either containing or immediately adjacent to the optic nerve. A minimum of eight retinas were analyzed per experimental time point. Variability of knockdown efficiency was low between animals. However, in all cases images were obtained from the central dorsal retina, equidistant from the optic nerve and marginal zone. For Table 1, GFAP-, PCNA-, and 4C4-positive cells were counted within a defined linear distance of 740 μm in the central dorsal retina. For Table 2, the number of TO-PRO-3-positive nuclei and GFAP-positive cells were counted within a defined linear distance of 340 μm confocal images obtained from eight dorsal retinas. Statistical significance was determined by ANOVA. Images were processed in Adobe Photoshop 7.0.

Cell Death Analysis

TUNEL assay was performed on frozen eye sections as previously described (Vihtelic et al., 2006) using the Apoptosis Detection Kit (R&D Systems, Minneapolis, MN). Eyes were fixed overnight in ethanolic formaldehyde and processed and sectioned as described above. Following rehydration in PBS, the tissue was permeabilized with Neuropore (R&D Systems). Incorporated biotinylated nucleotides were detected using a streptavidin-fluorescein conjugate. Analysis was performed using confocal microscopy. Ten micrometer z-series stacks (1 μm per stack) were captured from an area of the dorsal retina equidistant between the margin and the optic nerve. Images were processed in Adobe Photoshop 7.0 and pseudocolored to convert the green fluorescein to red.

Histology

Control and morpholino-electroporated light-lesioned eyes were fixed in 0.1M cacodylate/2.5% glutaraldehyde/2% formaldehyde for 24 h at 4°C. Eyes were dehydrated in an ethanol series and washed in a 1:1 xylene/ethanol and 100% xylene for 30 min. Eyes were infiltrated in a 1:1 xylene/Polybed 812 for 1 h and 1:2 xylene/Polybed 812 overnight at room temperature, and placed into Polybed 812 and polymerized for 48 h at 60°C. The eyes were sectioned (2.5 μm) and stained with 1% methylene blue/1% azure II as described (Vihtelic et al., 2006; Kassen et al., 2007). Images were taken of the dorsal retinal region.

RESULTS

Müller Glial Cells are the Source of Stem Cells in the Regenerating Retina During Constant Light Treatment

Data from multiple damage models indicate the Müller glia reenter the cell cycle following retinal insult and may represent the primary source of neuronal progenitors during zebrafish retinal regeneration (Wolburg, 1975; Vihtelic and Hyde, 2000; Yurco and Cameron, 2005; Fausett and Goldman, 2006; Raymond et al., 2006; Vihtelic et al., 2006; Bernardos et al., 2007; Fimbel et al., 2007). Using the *Tg*(*gfap*:*EGFP*)*nt11* line, which expresses EGFP specifically in the Müller glia (Kassen et al., 2007), we analyzed undamaged and light-treated retinas for the percentage of PCNA-positive cells that were EGFP-positive (Fig. 1 and Table 1). Although the presence PCNA-positive nuclei does not definitively indicate that cells are undergoing cell division, PCNA has been routinely used as a marker for cell proliferation in this and other systems (Vihtelic and Hyde, 2000; Leung et al., 2005; Thummel et al., 2006; Vihtelic et al., 2006; Fimbel et al., 2007; Kassen et al., 2007; Mahler and Driever, 2007).

Excluding the CGZ, we observed three separate classes of PCNA-positive cells in the undamaged retina [Fig. 1(A–C)]. The first class of PCNA-positive cells was observed in the ganglion cell layer (GCL). This class always colabeled with the microglial cell marker 4C4 and never colabeled with EGFP [Fig. 1(B) and Table 1]. The second class of PCNA-positive cells was confined to the outer nuclear layer (ONL) and did not colabel with EGFP or 4C4 [Fig. 1(C) and Table 1]. This class of cells most likely represented rod precursors (Hitchcock and Kakuk-Atkins, 2004). Finally, the third class of PCNA-positive cells was located in the INL and always colabeled with EGFP [Fig. 1(A–A″)]. Thus, the only proliferating INL cells in the undamaged, growing zebrafish retina were Müller glia. These data suggest the Müller glia represent the previously described INL stem cells that function to maintain neurogenesis of the adult teleost retina (Straznicky and Gaze, 1971; Johns and Easter, 1977; Fischer and Reh, 2001; Wu et al., 2001).

In the light-damaged retina, 49% of the EGFP-positive Müller glia have reentered the cell cycle after 36 h of constant light based on PCNA immunolocalization [Fig. 1(D,E) and

Table 1]. As we observed in the undamaged retina, every PCNA-positive INL cell at 36 h into the constant light treatment was an EGFP-expressing Müller glial cell. This demonstrated that the Müller glial cells, and not a separate stem cell population, are the source of the regenerated photoreceptors. The proliferating Müller glia generated PCNA-positive INL neuronal precursors that were clearly associated with the EGFP-positive Müller glia at 72 h of light treatment [Fig. 1(F)], but did not continue to express EGFP. These fusiform-shaped proliferating INL neuronal precursors migrated to the ONL [96 h, Fig. 1(G)], where they gave rise to both rod and cone photoreceptors (Vihtelic and Hyde, 2000; Wu et al., 2001; Bernardos et al., 2007). We devised an *in vivo* electroporation technique to knockdown PCNA during regeneration, and thus inhibited the generation of the neuronal precursors by preventing Müller glia cell divisions.

In Vivo Electroporation of Morpholinos into the Retina Does Not Cause Cell Death and Does Not Alter the Regeneration Response

An extensive series of controls were performed to ensure that the *in vivo* electroporation technique did not cause cell death or alter the photoreceptor regeneration response. The technique required the removal of the outer most component of the cornea, therefore, we first tested whether removal of this tissue drastically altered the cell proliferation or death response that characterizes the light damage-induced regeneration response. In light-treated retinas lacking the outermost corneal component, Müller glial cell division began at the same time point in both control and experimental retinas (data not shown). In addition, INL neuronal progenitor cell division and migration to the ONL also appeared normal when the outer most component of the cornea was removed (data not shown), indicating that removal of the corneal layer did not alter the time-course of light damage-induced INL cell proliferation necessary for retinal regeneration.

Next, we tested whether electroporation of morpholinos into the retina caused cell death as demonstrated by TUNEL [Fig. 2(A–C)]. We found a similar number of TUNEL-positive cells (<2 per section) both in the untreated retinas and in the retinas 24 h after electroporating with the Standard Control morpholino [Fig. 2(A,C)]. In contrast to untreated and electroporated retinas, retinas that were light-treated for 24 h exhibited large numbers of TUNEL-positive nuclei in the ONL, representing dying photoreceptors [Fig. 2(B)]. Thus, *in vivo* electroporation of morpholinos did not cause retinal cell death.

As an additional control for nonspecific toxic effects resulting from the morpholinos and/or the electroporation event, eyes were injected and electroporated with either the Standard Control morpholino, the two PCNA morpholinos, or the two 5-base mismatch control morpholinos, and subsequently analyzed after 1, 2, and 3 days of light treatment for the presence of HuC/D-positive amacrine and ganglion cells (Supplementary Fig. 1). All morphant retinas continued to exhibit relatively the same number of HuC/D-positive amacrine and ganglion cells at 1, 2, and 3 days of light treatment (Supplementary Fig. 1).

Finally, we tested whether electroporation of morpholinos into the retinas altered the regeneration response. Specifically, retinas electroporated with the Standard Control morpholino were compared with uninjected retinas at 1, 2, and 3 days of light treatment. Rod photoreceptor degeneration was analyzed by immunolocalization of rhodopsin, while neuronal progenitor proliferation and migration was assessed by immunolocalization of PCNA. We found comparable levels and distribution of rhodopsin and PCNA labeling between the uninjected retinas and the retinas injected and electroporated with either 5-base mismatch morpholino at 1, 2, and 3 days of light treatment [compare Fig. 2(A–C) and Fig. 2(D–I), respectively]. The use of the lissamine-tagged morpholino allowed us to confirm that the morpholinos persisted in all the retinal layers through 3 days of light treatment [Fig. 2(I′)].

Morpholinos Targeted Against PCNA Knockdown PCNA Levels in Zebrafish Embryos

During photoreceptor regeneration, *pcna* transcript levels increase (Kassen et al., 2007). To determine whether we could identify changes in PCNA protein expression, we compared PCNA protein levels at 0 and 96 h of light treatment by immunoblot analysis [Supplementary Fig. 2(A)]. The PCNA antibody identified a single protein band corresponding to the anticipated size of PCNA [Supplementary Fig. 2(A)]. In addition, the immunoblot analysis revealed a dramatic increase in the amount of PCNA protein at 96 h of light treatment compared with 0 h [Supplementary Fig. 2(A)].

We tested two nonoverlapping morpholinos targeted against *pcna* for their ability to knockdown PCNA expression in embryos. We injected each morpholino independently into one to four cell stage embryos. Uninjected and *pcna* morphant embryos were collected at 3 and 48 hpf for immunoblot analysis. The immunoblots demonstrated that PCNA is maternally expressed in the zebrafish embryo because protein was detected in zebrafish embryos at 3 hpf, which is prior to zygotic transcription initiation [Supplementary Fig. 2(B)]. Since translation-inhibiting morpholinos do not affect maternally loaded proteins, no differences in PCNA protein levels were observed between uninjected and morphant embryos at 3 hpf (data not shown). However, both *pcna* morpholinos effectively reduced zygotic PCNA expression by 48 hpf [Supplementary Fig. 2(B)], indicating both morpholinos could knockdown PCNA expression in the adult retina as well.

Injection and *In Vivo* Electroporation of PCNA Morpholino During Intense Light Exposure Inhibits Müller Glial Cell Division

The Müller glial cells undergo a robust proliferation response by 36 h of light exposure [Fig. 1(C,D)]. To determine the cellular consequences of blocking Müller glial cell division during the initial stages of photoreceptor regeneration, two nonoverlapping morpholinos targeted against *pcna* were selected. In addition, two 5-base mismatch control morpholinos, each corresponding to one of the two experimental *pcna* morpholinos, were utilized as controls for nonspecific electroporation and morpholino effects.

Dark-adapted adult *albino* zebrafish were injected and electroporated with either one of the *pcna* morpholinos (*pcna* MO1 and *pcna* MO2) or one of the two 5-base mismatch control morpholinos (see Fig. 3). At 1 day of light treatment, dorsal retinas injected and electroporated with either of the 5-base mismatch control morpholinos exhibited a few PCNA-positive cells in the ONL, similar to the uninjected light-treated control retinas [Fig. 3(A,D,G) arrows]. In contrast, PCNA-positive cells were not observed in the dorsal retinas injected and electroporated with either *pcna* morpholino [Fig. 3(J,M)]. Rhodopsin staining indicated that the rod outer segments were still organized and mostly intact in all the retinas at this stage in the light treatment. After 2 days of light, disorganized rhodopsin staining, which indicates significant damage to rod photoreceptors, was observed in all the uninjected and morphant retinas [Fig. 3(B,E,H,K,N)]. In addition, PCNA-positive cells were observed in the INL of uninjected retinas and those injected and electroporated with either 5-base mismatch control morpholino [Fig. 3(B,E,H) double arrowheads]. These INL-proliferating cells represent dividing Müller glia (see Fig. 1). In contrast, retinas injected and electroporated with either *pcna* morpholino lacked PCNA-positive cells [Fig. 3(K,N)], indicating that each of the *pcna* morpholinos effectively inhibited PCNA expression in the proliferating Müller glial cells following light damage. At 3 days of constant light treatment, a normal regenerative response was observed in the uninjected and the 5-base mismatch control retinas, including neuronal progenitor division and clusters of PCNA-positive cells migrating to the ONL [Fig. 3(C,F,I)]. Retinas injected and electroporated with either *pcna* morpholino continued to exhibit an absence of PCNA-positive nuclei [Fig. 3(L,O)]. Thus,

the anti-pcna morpholinos effectively blocked PCNA expression in the INL and ONL neuronal progenitors through 3 days of constant light treatment.

As an additional means of analyzing Müller glial-derived neuronal progenitors, we immunolabeled morphant retinas for the expression of phospho-histone H3 (H3P), which labels mitotically active cells, and Pax6, a retinal stem cell marker. At 3 days of light treatment, 5-base mismatch control retinas contained H3P-positive cells, whereas *pcna* morphant retinas did not (data not shown). This confirmed that PCNA knockdown resulted in blocking Müller glial cell proliferation. In addition to labeling mature amacrine and ganglion cells, Pax6 is upregulated in Müller glial-derived neuronal progenitors (Bernardos et al., 2007). We found that Pax6 colabeled with proliferating Müller glial-derived neuronal progenitors at 3 days of light treatment in 5-base mismatch control retinas [Fig. 4(C,D)], but never labeled neuronal progenitors in *pcna* morphant retinas [Fig. 4(E–H)]. Thus, PCNA knockdown prohibited the formation of Müller glial-derived Pax6-positive neuronal progenitors.

PCNA Knockdown Results in Decreased Glutamine Synthetase Levels, Loss of Mü ller Glial Processes, and Müller Glial Cell Death

Glutamine synthetase immunolocalizes to the Müller glia and clearly labels Müller glial processes spanning from the outer limiting membrane to the inner limiting membrane. After 2 days of constant light treatment, Standard Control morphant retinas and *pcna* morphant retinas contained glutamine synthetase-positive Müller glial cells [Fig. 5(A–C)]. During light treatment, Müller glial cells are activated and undergo cell hypertrophy (Vihtelic et al., 2006). Glutamine synthetase staining revealed this hypertrophy of the Müller glia in Standard Control morphant retinas after 3 days of light treatment [Fig. 5(D)]. The glutamine synthetase-positive glial cell processes appeared to be surrounding the clusters of neuronal progenitor cells [Fig. 5(D)]. In contrast, Müller glial cells in both *pcna* morphant retinas exhibited significantly decreased numbers and disorganized glutamine synthetase staining after 3 days of light treatment [Fig. 5(E,F)]. In these retinas, only a few Müller glial cell processes were observed.

To test whether the decrease in glutamine synthetase observed in *pcna* morphant retinas correlated with Müller glial cell death, Standard Control and *pcna* morphant retinas were analyzed after 2 days of light treatment for TUNEL [Fig. 5(G–I)]. Retinas injected and electroporated with the Standard Control morpholino exhibited TUNEL-positive nuclei in only the ONL, which corresponded to the light-induced photoreceptor cell death [Fig. 5(G)]. In contrast, retinas injected and electroporated with either *pcna* morpholino exhibited TUNEL-positive Müller glial cells after 2 days of light treatment [Fig. 5(H,I)], indicating that at least a subset of Müller glia underwent cell death following inhibition of proliferation. This is consistent with cell culture data demonstrating PCNA knockdown resulted in cell cycle arrest and subsequent apoptosis (Takase et al., 1992; Elliott et al., 2002; Choi et al., 2005; Gehen et al., 2007; Yu et al., 2006).

Long-Term Effects of PCNA Knockdown Include Müller Glial Cell Loss

PCNA knockdown resulted in death of at least a subset of Müller glial cells after 2 days of light treatment [Fig. 5(H,I)]. To determine the percentage of Müller glial cells that were lost as a result of PCNA knockdown, we analyzed uninjected and *pcna* morphant retinas for the presence of GFAP-positive Müller glial cells 28 days following light treatment termination (see Fig. 6). In addition to quantifying the number of Müller glial cells per visual field, the number of ONL, INL, and GCL cells were quantified (Table 1). We found no statistically significant difference in the total number of either INL or ganglion cell nuclei between the groups (Table 2). However, there were significantly more Müller glial cells in the uninjected

light-treated retinas than in *pcna* morphant retinas (Fig. 6 and Table 2). These data confirm that ~50% of Müller glial cells were targeted for cell death.

Inhibition of Mü ller Glial Cell Divisions Results in Failure of Rod and Cone Photoreceptor Regeneration

Rod photoreceptor nuclei are housed in the ONL. Twenty-eight days following light treatment, there were significantly fewer ONL nuclei in the *pcna* morphant retinas compared with uninjected retinas (Table 2, $p < 0.001$, $n = 5$). This suggested that the *pcna* morphant retinas cannot regenerate rod photoreceptors following light treatment. To confirm these results, we analyzed uninjected and *pcna* morphant retinas 28 days following light treatment by histology and immunohistochemistry.

Histological sections taken from uninjected light-treated retinas showed regenerated rod photoreceptors based on the thick appearance of the ONL and the fully extended rod outer segments [Fig. 7(A)]. In contrast, histological sections taken from light-treated *pcna* morphant retinas showed very few ONL nuclei and an absence of fully extended rod outer segments, indicating that rod photoreceptors had not fully regenerated [Fig. 7(B)]. Consistent with the histological data, immunolocalization demonstrated the *pcna* morphant retinas exhibited reduced rhodopsin expression, which was localized to a very sparse population of severely truncated rod outer segments [Fig. 8(E,F)]. In comparison, the uninjected and 5-base mismatch control morpholino retinas exhibited fully regenerated rhodopsin-containing rod outer segments [Fig. 8(B–D)].

We previosuly demonstrated that following light damage, regenerated cones appeared in patches with intervening spaces that lacked the cone cell type (Vihtelic and Hyde, 2000). We carefully analyzed serial retinal sections that were immunolabeled with UV and blue opsin antisera in the control and *pcna* morphant retinas. We found that cone cell regeneration was also affected by PCNA knockdown. Compared with uninjected and 5-base mismatch control retinas [Fig. 8(H–J,N–P)], *pcna* morphant retinas contained reduced numbers of UV opsin-expressing short single cones [Fig. 8(K,L)] and blue opsin-expressing long single cones [Fig. 8(Q,R)]. Together, these data strongly suggested that Müller glialderived neuronal progenitors never formed in *pcna* morphant retinas and showed that both rod and cone photoreceptors did not properly regenerate following PCNA knockdown.

DISCUSSION

We described a powerful approach to conditionally knockdown proteins of interest in the adult zebrafish retina. Using two independent morpholinos, we showed consistent knockdown of PCNA expression during 3 days of light treatment. This resulted in an inhibition of Müller glial cell division and subsequent Müller glial cell death. Consequently, the *pcna* morphant retinas lacked Pax6-positive neuronal precursors and did not regenerate rod and cone photoreceptors.

We tested multiple electroporation parameters (voltage drop, number of pulses, ms between pulses) before a successful electroporation protocol was determined. Previous electroporation studies in the regenerating zebrafish caudal fin reported multiple pulses at a very low voltage (15 V) (Thummel et al., 2006). Unlike the zebrafish fin, the retina is surrounded by multiple cell layers and is not readily accessible to tweezer electrodes. Thus, the parameters used in the fin were unsuccessful at efficiently electroporating morpholinos into the adult retina. Conversely, a high a voltage drop (100 V) often resulted in death of the organism. Finally, we found that 2 pulses of 75 V resulted in successful electroporation of the morpholinos without significantly harming the fish. These parameters were slightly less intense than the 5 pulses of 80 V recently described for electroporation of plasmid into the

mouse newborn pup retina (Matsuda and Cepko, 2004). Our parameters additionally required the removal of the outer most (or external-most) component of the cornea to increase electroporation efficiency. It is possible that increasing the number of pulses would eliminate the need for removal of this tissue. However, we chose to remove this structure to minimize the number of electroporation pulses.

Extensive control studies demonstrated the corneal dissection and electroporation failed to cause cell death or alter the cellular kinetics of the photoreceptor regeneration response. Specifically, we compared eyes with intact corneas to eyes that underwent corneal removal and found no difference in the onset of Müller glial cell proliferation or neuronal precursor proliferation and migration (data not shown). TUNEL analysis revealed that electroporation of the Standard Control morpholino did not cause cell death [Fig. 2(A–C)]. PCNA and rhodopsin immunolabeling demonstrated normal levels and distribution of neuronal precursors and rod photoreceptors during the light treatment in retinas electroporated with the Standard Control morpholino [Fig. 2(D–I)]. Finally, electroporation of two different 5-base mismatch control morpholinos failed to exhibit any toxic affects.

One of the strengths of this technique is the breadth of different retinal cell types that can be efficiently electroporated. For example, the PCNA knockdown inhibited proliferation of the Müller glial cells and the ONL rod precursor cells in the light-damaged retina [Fig. 3(B)]. We also successfully used this technique to knockdown EGFP expression from two different transgenes that are expressed in amacrine and ganglion cells (Thummel and Hyde, unpublished observations). While further tests will be necessary to determine if rod and cone photoreceptors can also be efficiently electroporated, these results indicate that a variety of retinal cell types can be targeted with this technique. One potential weakness was our inability to electroporate the morpholino throughout the entire retina. Because of the size and placement of the electrodes, we only electroporated the morpholino into the dorsal retina. This restricted electroporation field would limit the use of this technique in situations where the final assay requires a global assessment, such as the ERG analysis of retinal activity in response to light.

This technique could likely be used to study regeneration in other damage models (Wolburg, 1975; Vihtelic and Hyde, 2000; Wu et al., 2001; Hitchcock et al., 2004; Yurco and Cameron, 2005; Fausett and Goldman, 2006; Raymond et al., 2006; Fimbel et al., 2007). When the proliferation response is delayed several days, such as with ouabain-induced damage (Fimbel et al., 2007), it might be necessary to inject and electroporate the morpholino multiple times over several days, although the consequences of multiple electroporations on a single retina remain unclear. This technique could also be used to examine the function of proteins in intact adult retinas. For example, electroporation of morpholinos into the ganglion or amacrine cells that knockdown the expression of specific channels or signal transduction molecules could be used to study the function of these signaling pathways in visual processing.

We selected to knockdown PCNA expression during retinal regeneration for two reasons. First, PCNA knockdown served as a ‘‘test of principle’’ that *in vivo* electroporation of morpholinos into the regenerating retina is an efficient means of protein knockdown. Second, PCNA knockdown would provide insights to the potential role of Müller glial cell division during regeneration of the light-damaged retina. PCNA immunolocalization in the adult teleost retina was first described in the goldfish to identify proliferating rod precursor cells in the ONL (Negishi et al., 1990). Subsequent studies using neurotoxins specific to photoreceptors (i.e., tunicamycin) or subtypes of inner retinal neurons (i.e., 6-hydroxydopamine, 6-OHDA) demonstrated an increased number of PCNA-positive nuclei in both the INL and ONL (Negishi et al., 1991a,b). Coinjection of 6-OHDA and 5-

fluorouracil (5-FU), which blocks cell proliferation, resulted in a significantly reduced number of PCNA-positive cells in the ONL and retinal margins and a transient increase in the number of PCNA-positive cells in the contralateral control retina (Negishi, 1994). We failed to observe any effect of either the retinal injection or the electroporation on the cell death or proliferation in the contralateral control retina. This suggests that any effects resulting from the morpholino knockdown are restricted to the experimental retina. Additionally, our studies focused on the Müller glial and INL neuronal progenitor cell populations, which serve as the source of the regeneration response. Furthermore, because studies using 5-FU to inhibit cell division following tunicamycin-induced photoreceptor damage were not reported, this study represents the first report of cell cycle inhibition following photoreceptor damage.

Several studies provide insight to the Müller glial cell's role in retinal regeneration. Müller glial cell proliferation and subsequent differentiation into specific retinal cell classes following damage was first demonstrated in the chick retina (Fischer and Reh, 2001). Subsequently, several published reports using the adult zebrafish retina demonstrated that the Müller glia begin to proliferate in response to a variety of retinal insults, and that these glial cells serve as the source for the regeneration of different neuronal classes in the regenerated retina (Yurco and Cameron, 2005; Fausett and Goldman, 2006; Raymond et al., 2006; Bernardos et al., 2007). In addition, a limited regenerative response, in which proliferating Müller glia serve as a source of new neurons, has recently been reported in mammalian retinas (Ooto et al., 2004; Das et al., 2006). Thus, given the importance of the Müller glia in retinal regeneration, it is not surprising that inhibiting Müller glia proliferation results in regeneration arrest.

PCNA knockdown resulted in three significant findings regarding the role of the Müller glia during retinal regeneration. First, the selective *in vivo* targeting of Müller glia to undergo apoptosis following PCNA knockdown is a novel finding. Cell culture studies have shown the potential for PCNA knockdown to lead to G1 arrest and cell death (Takase et al., 1992; Elliott et al., 2002; Choi et al., 2005; Gehen et al., 2007; Yu et al., 2006). Here we show an *in vivo* example of this proliferation arrest leading to cell death with the Müller glia. This suggests that the Müller glial receive a signal to reenter the cell cycle, at which point they become committed to proliferate. In the failure to proliferate, the committed Müller glial cells must apoptose. Furthermore, not all Müller glial cells are targeted for cell death following PCNA knockdown. We hypothesize that only those Müller glial cells that attempt to divide at 36 h of light treatment are targeted for cell death. Cell counts from dorsal retinas support this hypothesis, as half of the total population of Mü0ler glial cells divide at 36 h in light-treated control retinas, and half are still present at 28 days post-light treatment in PCNA knockdown retinas (Tables 1 and 2). The second novel finding of this study is the severe decrease and disruption of the rod and cone photoreceptors in *pcna* morphant retinas 28 days following light treatment. Because of the positioning of the electrodes around the eye, we efficiently electroporated the morpholino into the dorsal portion of the retina without knocking-down PCNA expression in the circumferential marginal zone. Yet, we did not observe significant regeneration of Müller glia and rod and cone photoreceptors across the dorsal region of the light-damaged retina (Fig. 8 and Table 2). This clearly demonstrates that the neuronal stem cells that exist in the circumferential marginal zone cannot make a significant contribution to the retinal regeneration response. Furthermore, the rod precursor cells in the ONL, which could also contribute to the regeneration of rod photoreceptors, were also effectively inhibited from proliferation in the *pcna* morphants. Thus, these data provide strong evidence that the Müller glia are the only source of neuronal progenitors in the light-damage model. Furthermore, because these data demonstrate that cell division is a requirement for photoreceptor regeneration, they eliminate the mechanisms where the Müller glia simply dedifferentiate into neuronal progenitors or trans-differentiate into

neurons. This leaves the induction of increased Müller glial cell proliferation, which generates the pluripotent neuronal progenitor cells as the likely mechanism of photoreceptor replacement. Finally, based on these and other knockdown studies, we determined that *in vivo* electroporation of morpholinos into the regenerating zebrafish retina will only efficiently knockdown the protein of interest for 4–5 days (data not shown). This is similar to the length of time morpholinos are effective during zebrafish embryogenesis, and implies that once the window of protein knockdown has passed, the retinas could ‘‘recover’’. However, the near complete lack of regenerated rod and cone photoreceptors at 28 days post-light treatment shows that this does not occur in PCNA knockdown retinas. Thus, these data suggest there is a window of time to signal the Müller glia to proliferate and once that window has expired, the opportunity for the Müller glia to proliferate is lost.

As demonstrated by the efficiency of PCNA knockdown and the variety of techniques available to analyze the *pcna* morphant phenotype, this approach holds much promise for testing the function of other proteins of interest during retinal regeneration. Recently, two microarray analyses were reported that compare gene expression changes during the regeneration of either a surgically-excised retinal patch or the light-damaged retina (Cameron et al., 2005; Kassen et al., 2007). These two studies revealed numerous gene expression changes that likely correspond to different events that occur during retinal regeneration, such as the signals to initiate Müller glial cell proliferation, the migration of the neuronal progenitors to the damaged retinal layer, and the differentiation of the correct neuronal cell type. While comparing these two microarray data sets may reveal interesting and important candidate genes, ultimately these genes and their encoded proteins must be tested for potential function during regeneration. As we demonstrated with the PCNA knockdown, the electroporation of morpholinos provides a relatively rapid method to test these candidate genes and can generate robust phenotypes that can be easily studied.

Supplementary Material

Refer to Web version on PubMed Central for supplementary material.

Acknowledgments

The authors would like to thank the Freimann Life Science Center staff for the excellent care and maintenance of the zebrafish. We thank Dr. Thomas Vihtelic for comments on the manuscript, members of the Hyde lab for discussions during this work, and Suzyanne Guzicki for excellent technical assistance in generating the *Tg(gfap:EGFP)nt11* transgenic line.

Contract grant sponsor: National Institutes of Health; contract grant number: R21-EY017134.

Contract grant sponsors: Center for Zebrafish Research at the University of Notre Dame, Fight For Sight fellowship.

REFERENCES

Bernardos RL, Barthel LK, Meyers JR, Raymond PA. Late-stage neuronal progenitors in the retina are radial Muller glia that function as retinal stem cells. J Neurosci. 2007; 27:7028–7040. [PubMed: 17596452]

Cameron DA, Gentile KL, Middleton FA, Yurco P. Gene expression profiles of intact and regenerating zebrafish retina. Mol Vis. 2005; 11:775–791. [PubMed: 16205622]

Choi HJ, Choi YH, Yee SB, Im E, Jung JH, Kim ND. Ircinin-1 induces cell cycle arrest and apoptosis in SK-MEL-2 human melanoma cells. Mol Carcinog. 2005; 44:162–173. [PubMed: 16163705]

Das AV, Mallya KB, Zhao X, Ahmad F, Bhattacharya S, Thoreson WB, Hegde GV, et al. Neural stem cell properties of Muller glia in the mammalian retina: Regulation by Notch and Wnt signaling. Dev Biol. 2006; 299:283–302. [PubMed: 16949068]

Detrich, HW.; Westerfield, M.; Zon, LI. Methods in Cell Biology: The Zebrafish Biology. New York: Academic Press; 1999.

Elliott MJ, Stilwell A, Dong YB, Yang HL, Wong SL, Wrightson WR, Martin RC, et al. C-terminal deletion mutant p21(WAF1/CIP1) enhances E2F-1-mediated apoptosis in colon adenocarcinoma cells. Cancer Gene Ther. 2002; 9:453–463. [PubMed: 11961668]

Fausett BV, Goldman D. A role for alpha1 tubulin-expressing Muller glia in regeneration of the injured zebrafish retina. J Neurosci. 2006; 26:6303–6313. [PubMed: 16763038]

Fimbel SM, Montgomery JE, Burket CT, Hyde DR. Regeneration of inner retinal neurons after intravitreal injection of ouabain in zebrafish. J Neurosci. 2007; 27:1712–1724. [PubMed: 17301179]

Fischer AJ, Reh TA. Muller glia are a potential source of neural regeneration in the postnatal chicken retina. Nat Neurosci. 2001; 4:247–252. [PubMed: 11224540]

Gehen SC, Vitiello PF, Bambara RA, Keng PC, O'Reilly MA. Down-regulation of PCNA potentiates p21-mediated growth inhibition in response to hyperoxia. Am J Physiol Lung Cell Mol Physiol. 2007; 292:716–724.

Hagedorn M, Fernald RD. Retinal growth and cell addition during embryogenesis in the teleost, *Haplochromis burtoni* . J Comp Neurol. 1992; 321:193–208. [PubMed: 1380013]

Hitchcock P, Kakuk-Atkins L. The basic helix-loop-helix transcription factor neuroD is expressed in the rod lineage of the teleost retina. J Comp Neurol. 2004; 477:108–117. [PubMed: 15281083]

Hitchcock P, Ochocinska M, Sieh A, Otteson D. Persistent and injury-induced neurogenesis in the vertebrate retina. Prog Retin Eye Res. 2004; 23:183–194. [PubMed: 15094130]

Johns PR, Easter SS Jr. Growth of the adult goldfish eye. II. Increase in retinal cell number. J Comp Neurol. 1977; 176:331–341. [PubMed: 915041]

Kassen SC, Ramanan V, Montgomery JE, Burket TC, Liu CG, Vihtelic TS, Hyde DR. Time course analysis of gene expression during light-induced photoreceptor cell death and regeneration in albino zebrafish. Dev Neu-robiol. 2007; 67:1009–1031.

Leung AY, Leung JC, Chan LY, Ma ES, Kwan TT, Lai KN, Meng A, et al. Proliferating cell nuclear antigen (PCNA) as a proliferative marker during embryonic and adult zebrafish hematopoiesis. Histochem Cell Biol. 2005; 124:105–111. [PubMed: 16028068]

Mahler J, Driever W. Expression of the zebrafish intermediate neurofilament Nestin in the developing nervous system and in neural proliferation zones at postem-bryonic stages. BMC Dev Biol. 2007; 7:89. [PubMed: 17651502]

Marcus RC, Delaney CL, Easter SS Jr. Neurogenesis in the visual system of embryonic and adult zebrafish (*Danio rerio*). off. Vis Neurosci. 1999; 16:417–424. [PubMed: 10349963]

Matsuda T, Cepko CL. Electroporation and RNA interference in the rodent retina in vivo and in vitro. Proc Natl Acad Sci USA. 2004; 101:16–22. [PubMed: 14603031]

Nasevicius A, Ekker SC. Effective targeted gene ''knockdown'' in zebrafish. Nat Genet. 2000; 26:216–220. [PubMed: 11017081]

Negishi K. 5-Fluorouracil reduces proliferating cell nuclear antigen immunoreactive cells in goldfish retina. Neurosci Res. 1994; 19:21–29. [PubMed: 7911984]

Negishi K, Stell WK, Takasaki Y. Early histogenesis of the teleostean retina: Studies using a novel immuno-chemical marker, proliferating cell nuclear antigen (PCNA/cyclin). Brain Res Dev Brain Res. 1990; 55:121–125.

Negishi K, Stell WK, Teranishi T, Karkhanis A, Owusu-Yaw V, Takasaki Y. Induction of proliferating cell nuclear antigen (PCNA)-immunoreactive cells in goldfish retina following intravitreal injection with 6-hy-droxydopamine. Cell Mol Neurobiol. 1991; 11:639–659. [PubMed: 1685943]

Negishi K, Sugawara K, Shinagawa S, Teranishi T, Kuo CH, Takasaki Y. Induction of immunoreactive proliferating cell nuclear antigen (PCNA) in goldfish retina following intravitreal injection with tunicamycin. Brain Res Dev Brain Res. 1991; 63:71–83.

Ooto S, Akagi T, Kageyama R, Akita J, Mandai M, Honda Y, Takahashi M. Potential for neural regeneration after neurotoxic injury in the adult mammalian retina. Proc Natl Acad Sci USA. 2004; 101:13654–13659. [PubMed: 15353594]

Raymond PA, Barthel LK, Bernardos RL, Perkowski JJ. Molecular characterization of retinal stem cells and their niches in adult zebrafish. BMC Dev Biol. 2006; 6:36. [PubMed: 16872490]

Shi X, Bosenko DV, Zinkevich NS, Foley S, Hyde DR, Semina EV, Vihtelic TS. Zebrafish pitx3 is necessary for normal lens and retinal development. Mech Dev. 2005; 122:513–527. [PubMed: 15804565]

Straznicky K, Gaze RM. The growth of the retina in *Xenopus laevis*: An autoradiographic study. J Embryol Exp Morphol. 1971; 26:67–79. [PubMed: 5565078]

Takase K, Sawai M, Yamamoto K, Yata J, Takasaki Y, Teraoka H, Tsukada K. Reversible G1 arrest induced by dimethyl sulfoxide in human lymphoid cell lines: Kinetics of the arrest and expression of the cell cycle marker proliferating cell nuclear antigen in Raji cells. Cell Growth Differ. 1992; 3:515–521. [PubMed: 1356417]

Thummel R, Bai S, Sarras MP Jr, Song P, McDermott J, Brewer J, Perry M, et al. Inhibition of zebrafish fin regeneration using in vivo electroporation of morpholinos against fgfr1 and msxb. Dev Dyn. 2006; 235:336–346. [PubMed: 16273523]

Thummel R, Li L, Tanase C, Sarras MP Jr. Godwin AR. Differences in expression pattern and function between zebrafish hoxc13 orthologs: Recruitment of Hoxc13b into an early embryonic role. Dev Biol. 2004; 274:318–333. [PubMed: 15385162]

Vihtelic TS, Doro CJ, Hyde DR. Cloning and characterization of six zebrafish photoreceptor opsin cDNAs and immunolocalization of their corresponding proteins. Vis Neurosci. 1999; 16:571–585. [PubMed: 10349976]

Vihtelic TS, Hyde DR. Light-induced rod and cone cell death and regeneration in the adult albino zebrafish (*Danio rerio*) retina. J Neurobiol. 2000; 44:289–307. [PubMed: 10942883]

Vihtelic TS, Soverly JE, Kassen SC, Hyde DR. Retinal regional differences in photoreceptor cell death and regeneration in light-lesioned albino zebrafish. Exp Eye Res. 2006; 82:558–575. [PubMed: 16199033]

Wei X, Cheng Y, Luo Y, Shi X, Nelson S, Hyde DR. The zebrafish Pard3 ortholog is required for separation of the eye fields and retinal lamination. Dev Biol. 2004; 269:286–301. [PubMed: 15081374]

Westerfield, M. The Zebrafish Book: A Guide for the Laboratory Use of Zebrafish (*Danio rerio*). Eugene, OR: University of Oregon Press; 1995.

Wolburg H. Time- and dose-dependent influence of ouabain on the ultrastructure of optic neurones. Cell Tissue Res. 1975; 164:503–517. [PubMed: 1203964]

Wu DM, Schneiderman T, Burgett J, Gokhale P, Barthel L, Raymond PA. Cones regenerate from retinal stem cells sequestered in the inner nuclear layer of adult goldfish retina. Invest Ophthalmol Vis Sci. 2001; 42:2115–2124. [PubMed: 11481280]

Yu J, Qiao L, Zimmermann L, Ebert MP, Zhang H, Lin W, Rocken C, et al. Troglitazone inhibits tumor growth in hepatocellular carcinoma in vitro and in vivo. Hepatology. 2006; 43:134–143. [PubMed: 16374840]

Yurco P, Cameron DA. Responses of Muller glia to retinal injury in adult zebrafish. Vision Res. 2005; 45:991–1002. [PubMed: 15695184]

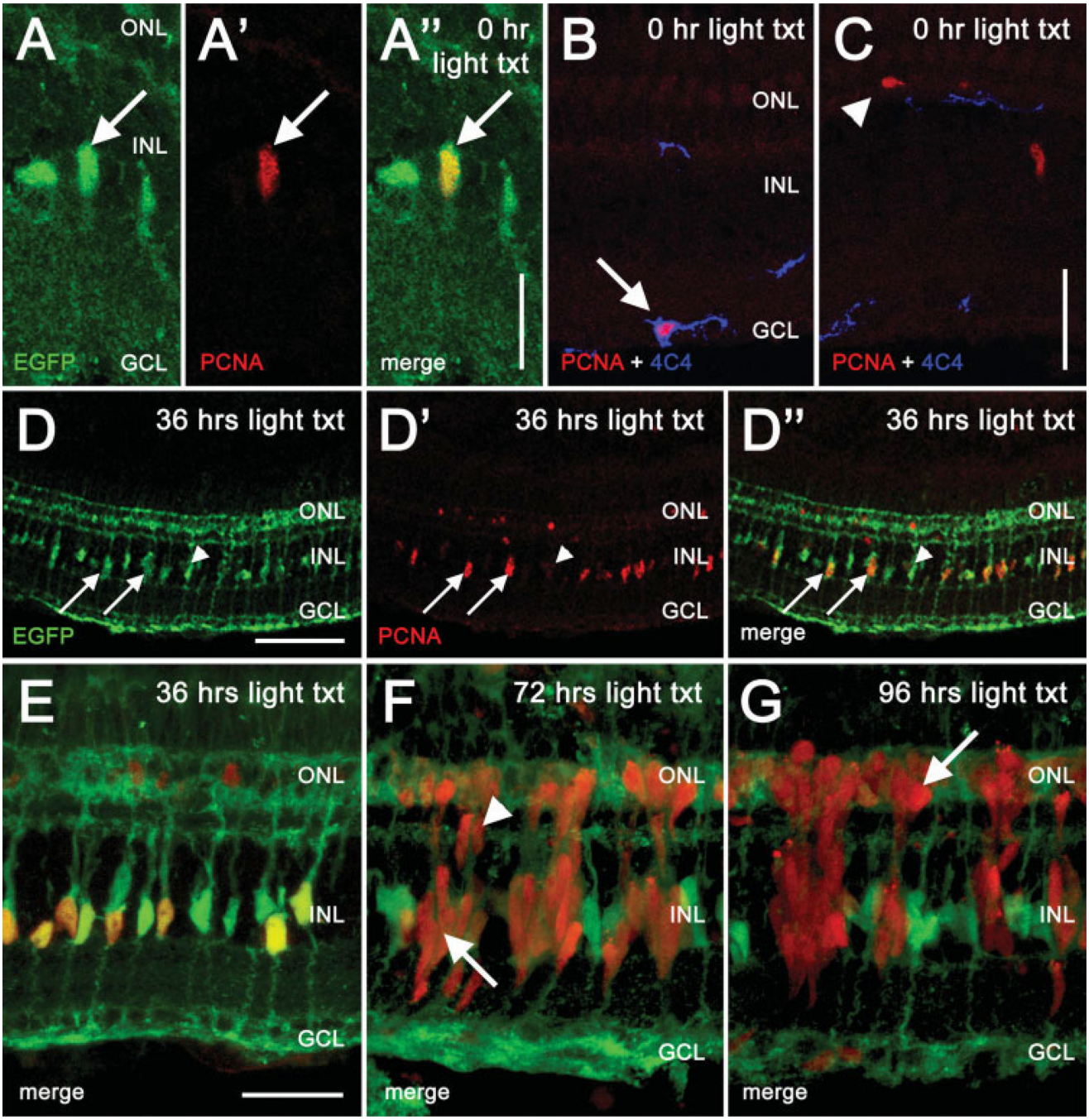

Figure 1.

Localization of PCNA in the *Tg*(*gfap:EGFP*)*nt11 albino* zebrafish retina during light treatment. EGFP expression in the Müller glial cells in the *Tg*(*gfap:EGFP*)*nt11 albino* zebrafish was examined relative to PCNA immunolocalization during the intense light treatment. In the control (0 h, panels A and B), PCNA expression was rarely observed and was restricted to three cell types: EGFP-expressing Müller glial cells in the INL (panels A′ and A″, arrow), 4C4-positive microglia cells located near the GCL (panel B, arrow), and resident rod precursor cells in the ONL (panel C, arrowhead). At 36 h (panels D and E), PCNA expression is detected in large numbers of the INL nuclei and it colocalizes with the EGFP expression in the Müller glial cells (panels D–D″, arrows). Not all Müller glial cells

are PCNA-positive (panels D–D″, arrowhead). At 72 h, the EGFP-expressing Müller glial cells no longer colabel with PCNA (panel F, arrow). However, PCNA-positive neuronal progenitors have begun to migrate from the INL to the ONL along the Muüller glial processes (panel F, arrowhead). At 96 h, large numbers of PCNA-positive progenitors populate the ONL (panel G, arrow). These results suggest the initial Müller cell proliferation event, which occurs subsequent to the light-induced photoreceptor damage, produces a population of neuronal progenitor cells that continue to proliferate. Scale bars: panel A″, 12 μm (panels A–A″); panel C (B–C), 25 μm; panel D, 100 μm (D–D″); panel E, 25 μm (E–G).

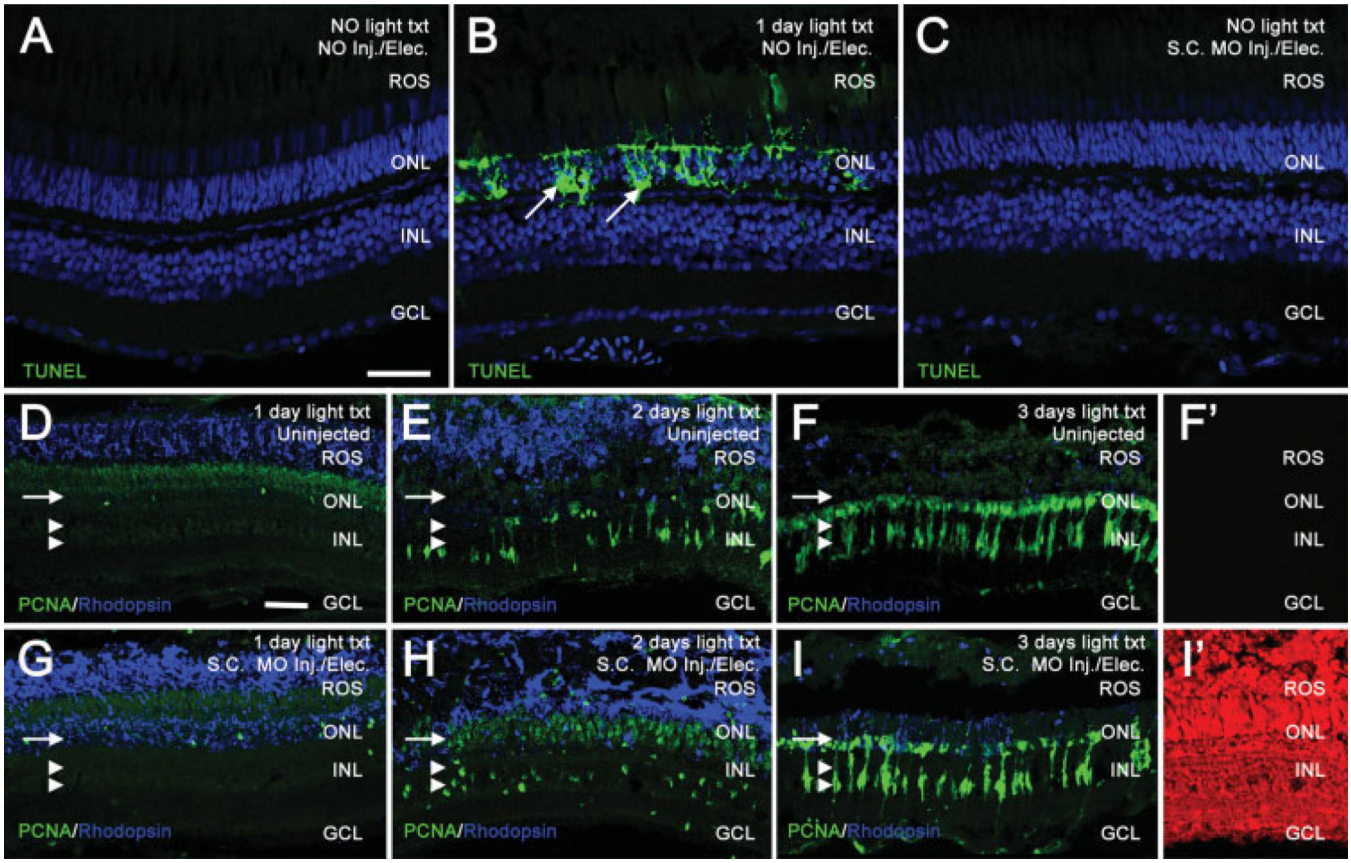

Figure 2.

In vivo electroporation of morpholinos into the zebrafish retina does not cause cell death or adversely affect the regeneration response. TUNEL assays were used to compare cell death between uninjected, 24 h light-treated, and electroporated retinas (panels A–C). TO-PRO-3 (shown in blue) was used to stain nuclei. In uninjected, nonlight treated retinas, TUNEL labeling (shown in green) was not observed (panel A). In contrast, retinas light-treated for 24 h exhibited large amounts of TUNEL-positive nuclei in the ONL, representing dying photoreceptors (panel B, arrows). Non light-treated retinas electroporated with a Standard Control morpholino exhibited no detectable TUNEL labeling 24 h following electroporation (panel C), similar to uninjected control retinas. Uninjected retinas (panels D–F) and Standard Control electroporated retinas (panels G–I) were analyzed for PCNA (shown in green) and rhodopsin (shown in blue) immunolocalization. Panels D–F show the normal regenerative response at 1, 2, and 3 days of light, respectively. Rhodopsin decreases as rod photoreceptors degenerate. PCNA-positive, Müller glial derived, neuronal progenitors increase over the timecourse in both the INL (panels D–F, double arrowheads) and the ONL (panels D–F, arrow). Panel F′ shows background levels of red autofluorescence in uninjected retinas at 3 days of light treatment. Panels G–I show the normal regenerative response in retinas electroporated with a Standard Control morpholino. Similar to uninjected retinas, rhodopsin decreases and PCNA increases throughout the timecourse in both the INL (panels G–I, double arrowheads) and the ONL (panels G–I, arrow), indicating that electroporation does not adversely affect the regenerative response. Panel I′ shows a high level of lissamine-tagged Standard Control morpholino in all retinal layers at 3 days of light treatment. Scale bars: panel A, 25 μm (A–C); panel D, 25 μm (D–I′).

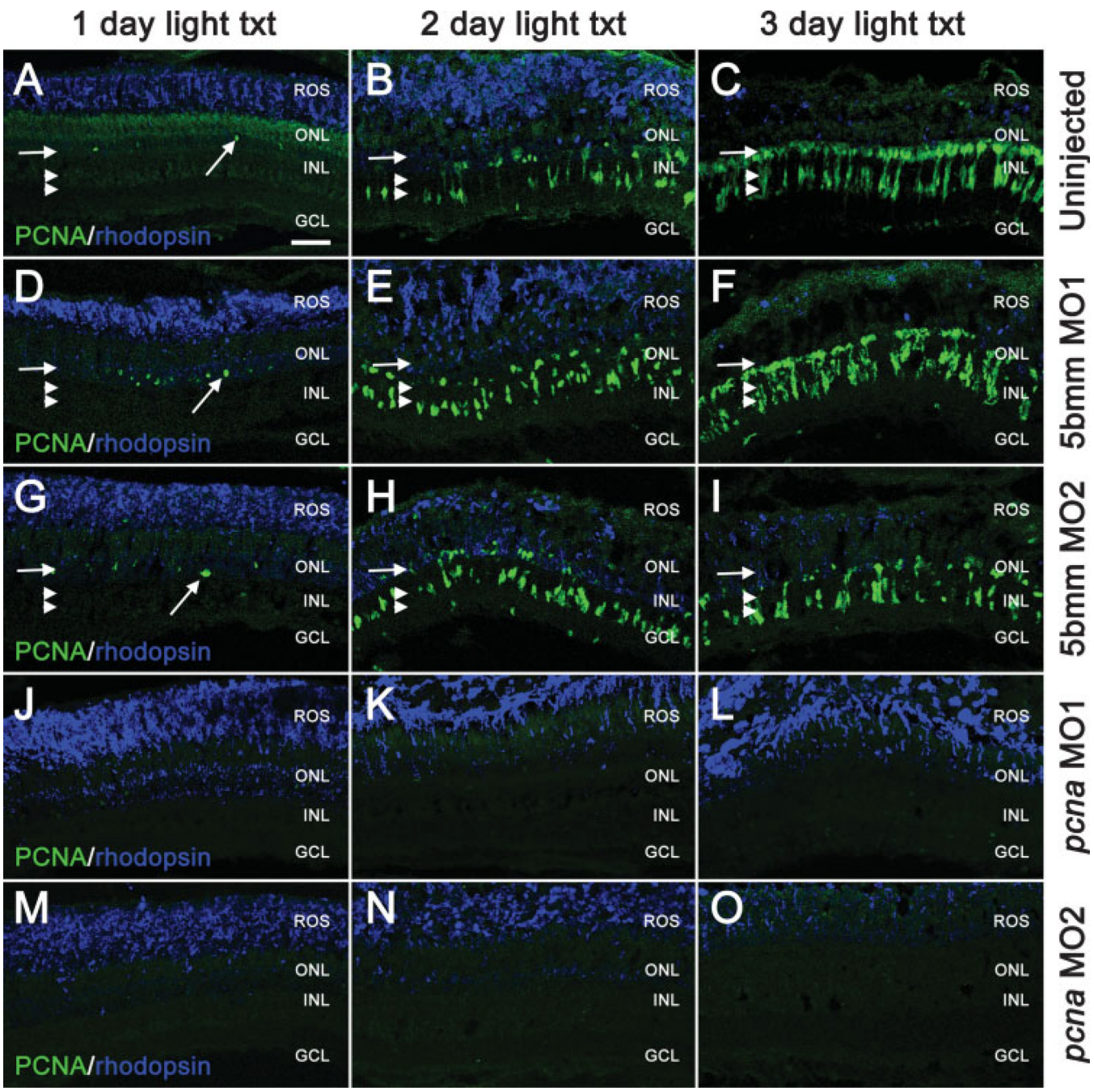

Figure 3.

Injection and *in vivo* electroporation of *pcna* morpholino during constant light exposure knocks down PCNA levels. Dark-adapted adult *albino* zebrafish were injected and electroporated with either the *pcna* morpholino 1 (*pcna* MO1), *pcna* morpholino 2 (pcna MO2), 5-base mismatch morpholino 1 (5bmm MO1), or 5-base mismatch morpholino 2 (5bmm MO2) and exposed to constant intense light. Retinas were harvested at 1, 2, and 3 days into the light treatment and immunolabeled with PCNA (shown in green) and rhodopsin (shown in blue). In the uninjected control retinas (panels A–C) and the 5-base mismatch control retinas (panels D–I), light exposure results in a progressive accumulation of PCNA-positive cells within the INL and ONL and a loss of rhodopsin. Arrows and

double arrowheads indicate the relative positions of the PCNA-positive cells in the ONL and in INL, respectively. In contrast, the *pcna* morphant retinas lack any PCNA-positive cells throughout the light exposure (Panels J–O). Scale bar: panel A, 25 μm (A–O).

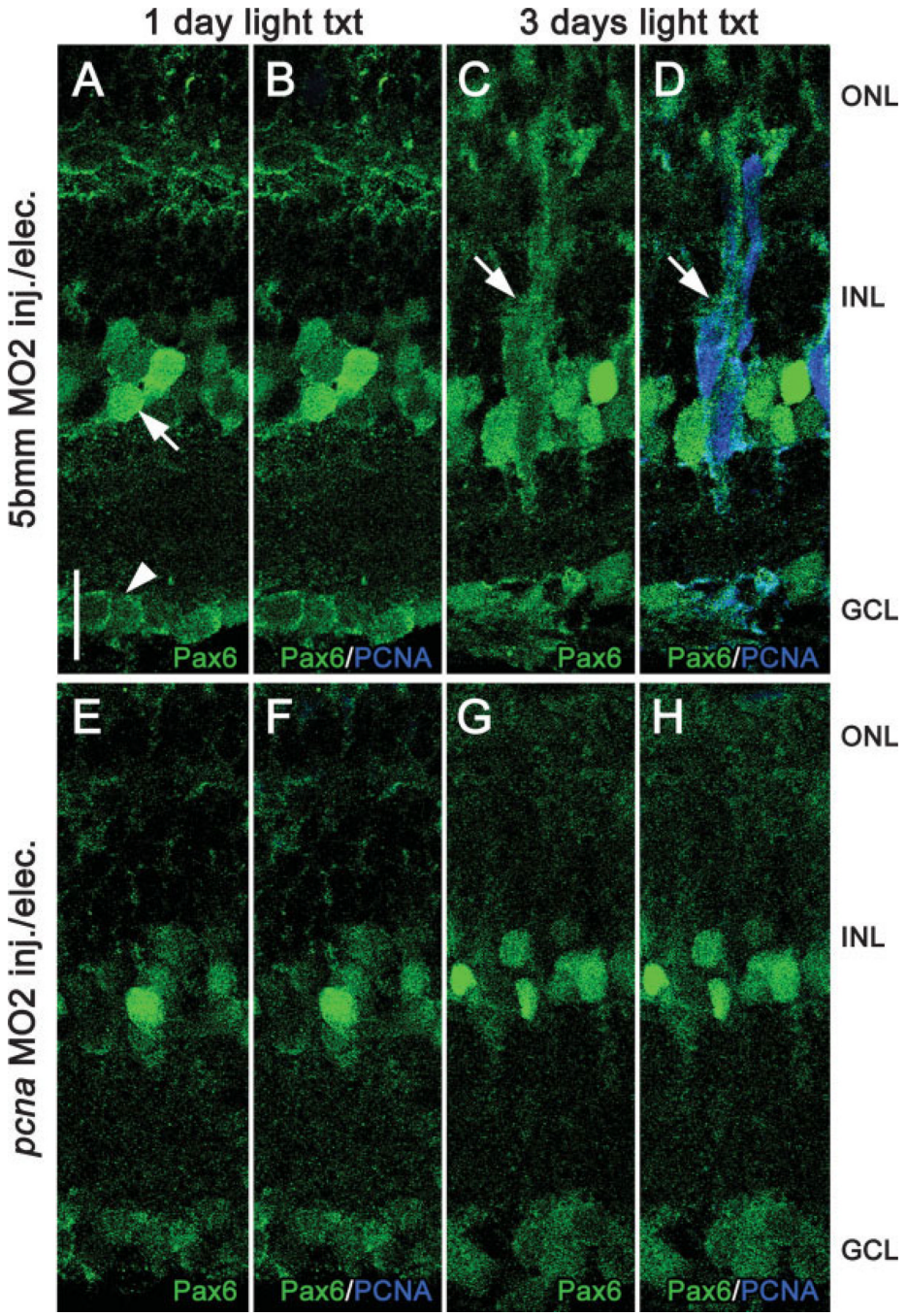

Figure 4.

pcna morphant retinas lack Pax6-positive neuronal progenitors. Pax6 immunolocalization (shown in green) was performed to test whether neuronal progenitors are generated in *pcna* morphant retinas. Pax6 labels retinal neuronal progenitors and mature amacrine and ganglion cells (Bernardos et al., 2007). At 1 day of light treatment, 5-base mismatch control retinas (Panels A and B) exhibited Pax6 immunolocalization in mature amacrine (panel A, arrow) and ganglion cells (panel A, arrowhead). At 3 days of light treatment, following Müller glial cell division, 5-base mismatch control retinas exhibited Pax6 expression in Muüller glial-derived neuronal progenitors (panel C, arrow), which colabeled with PCNA (panel D, shown in blue). Similar to control retinas, *pcna* morphant retinas (panels E–H)

exhibited Pax6-positive mature amacrine and ganglion cells at 1 day (panels E and F) and 3 days (panels G and H) of light treatment. However, the large and diffusely stained Pax6-postitive neuronal precursors were never detected in *pcna* morphant retinas (panels G and H). Scale bar: panel A, 10 μm (A–I).

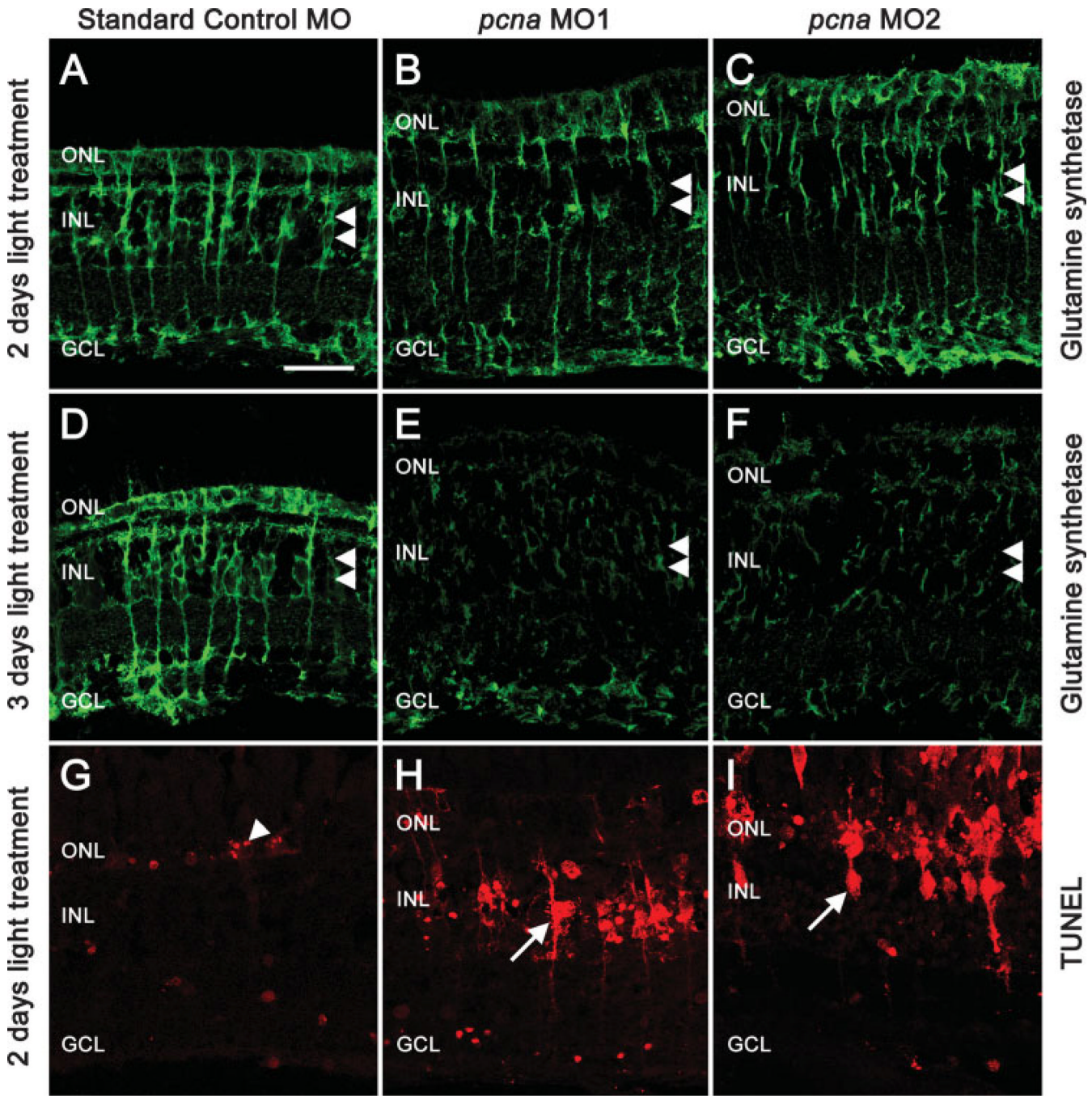

Figure 5.

PCNA knockdown results in decreased glutamine synthetase levels, loss of Müller glial processes, and Müller glial cell death. Dark-adapted adult *albino* zebrafish were injected and electroporated with the Standard Control morpholino, *pcna* morpholino 1 (*pcna* MO1), or *pcna* morpholino 2 (*pcna* MO2), and placed in constant light. Retinas were harvested after either 2 or 3 days and processed to immunolocalize glutamine synthetase (green), which labels Müller glial cell nuclei housed in the INL (panels A–F, double arrowheads) and Müller glial cell processes extending to the ONL and GCL. The retinas injected and electroporated with the Standard Control morpholino exhibit robust glutamine synthetase expression in the Muüler cells (Panels A and D). The *pcna* morphant retinas exhibited a

disruption of Müller glial cell morphology and a reduction of glutamine synthetase expression (Panels B, C, E, and F). To test for Muüller glia cell death, the retinas were immunolabeled with TUNEL (Panels G–I; red). The TUNEL-positive cells (arrowheads) in the control retina were primarily restricted to the outer nuclear layer (ONL), which is consistent with light-damaged photoreceptors (Panel G). However, *pcna* morphant retinas exhibited many TUNEL-positive cells in the INL (Panels H and I, arrows), which possess processes like Muüller glial cells. Scale bar: panel A, 25 μm (A–I).

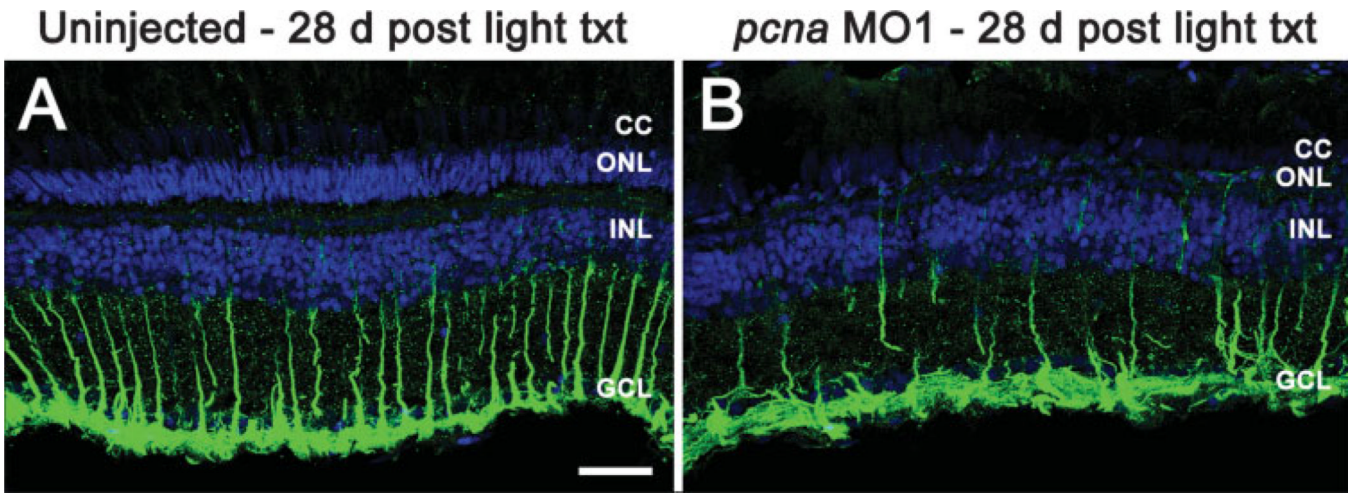

Figure 6.

PCNA knockdown results in a reduced number of Müller glial cells 28 days post light treatment. To determine the number of Müller glial cells, GFAP (green) was immunolocalized at 28 days following constant light treatment. Uninjected control retinas (panel A) exhibited Müller glial cell processes extending from the inner nuclear layer (INL) beyond the ganglion cell layer (GCL) to the inner limiting membrane. In contrast, *pcna* morphant retinas contained fewer numbers of GFAP-positive Müller glial cell processes (panel B). TO-PRO-3 counter-staining of retinas labeled cell nuclei in blue. Scale bar: panel A, 25 μm (A–B).

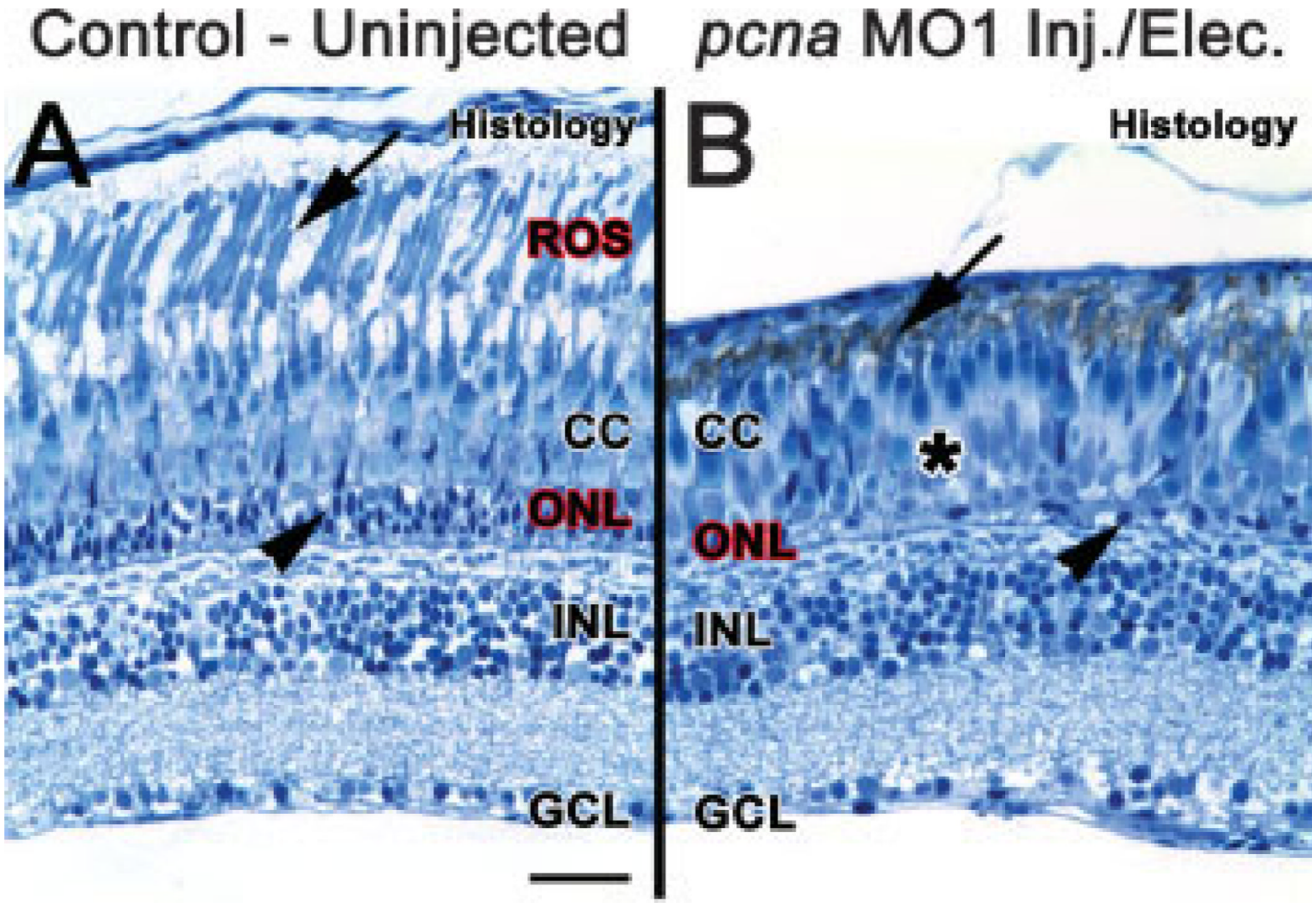

Figure 7.

PCNA knockdown results in a reduction of ROS and ONL nuclei 28 days post light treatment. At 28 days following constant light treatment, histological sections of uninjected retinas (panel A) showed a regenerated outer nuclear layer (ONL, arrowhead), cone cell layer (CC) and rod outer segments (ROS, arrow). In contrast, histological sections from *pcna* morphant retinas (panel B) showed an absence of distinguishable ROS (arrow), very few nuclei present in the ONL (arrowhead), a disorganized cone cell layer, and large sections absent of long single cones (asterisk). Scale bar: panel A, 25 μm (A–B).

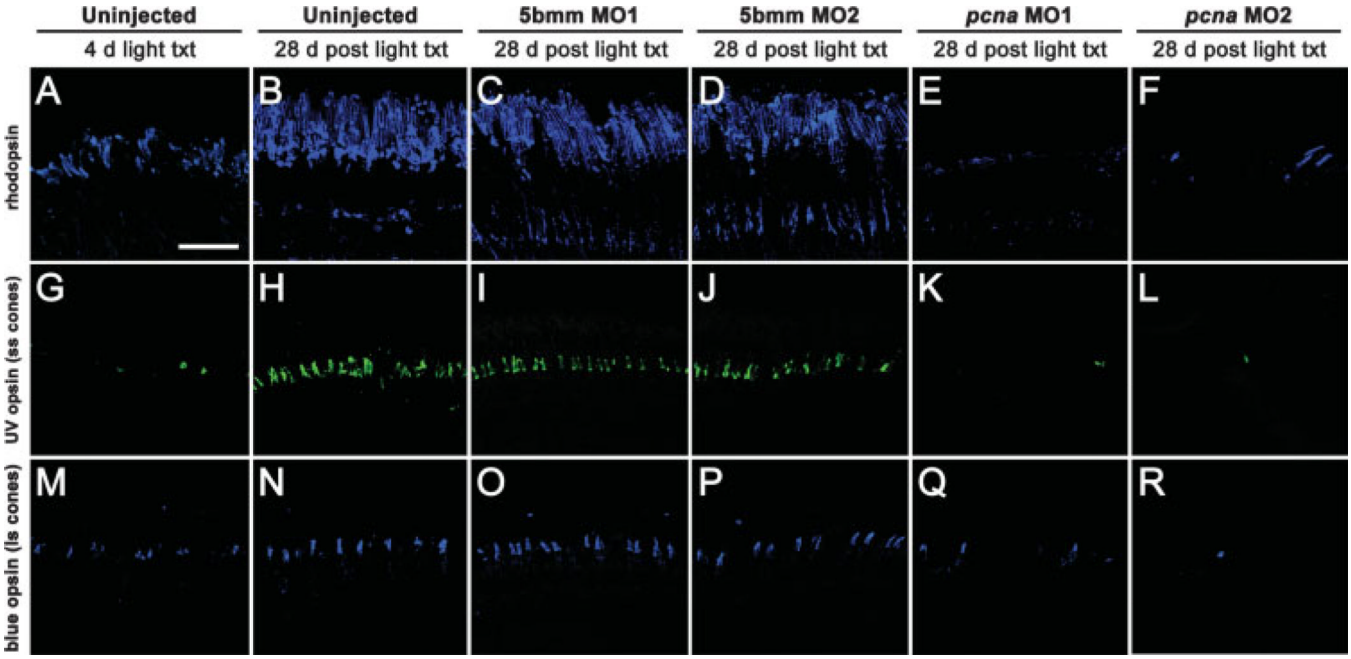

Figure 8.

PCNA knockdown results in a reduction and disorganization of photoreceptors 28 days post light treatment. Rhodopsin immunolabeled rod outer segments, UV opsin immunolabeled short single cone outer segments (ss cones), and blue opsin immunolabeled long single cone outer segments (ls cones). Following 4 days of constant light treatment, uninjected control retinas exhibited reduced numbers and disorganized rod (panel A) and cone outer segments (panels G and M). However, by 28 days post light treatment, uninjected retinas regenerated both rod and cone outer segments (panels B, H, and N). 5-base mismatch control retinas, using either 5-base mismatch morpholino 1 (5bmm MO1) or 5-base mismatch morpholino 2 (5bmm MO2), showed a similar regeneration of rod and cone photoreceptors at 28 days post light treatment (panels C, D, I, J, O, and P). In contrast, *pcna* morphant retinas, using either *pcna* morpholino 1 (*pcna* MO1) or *pcna* morpholino 2 (*pcna* MO2), exhibited greatly reduced numbers of rod outer segments (panels E and F, arrows). In addition, cone photoreceptors were also present in greatly reduced numbers in *pcna* morphant retinas (panels K, L, Q, and R). Scale bar: panel A, 50 μm (A–R).

Table 1

Analysis of Cell Proliferation at 0 and 36-h Light Treatment

		Retinal Layers	Average No. of PCNA Cells	GFAP+ (%)	4C4+ (%)
0-h light treatment	*N* = 24 retinas	ONL	1.1 (1.3)	0	0
		INL	0.1 (0.3)	100	0
		GCL	0.1 (0.3)	0	100
36-h light treatment	*N* = 10 retinas	ONL	12.1 (5.7)	0	
		INL	27.7 (6.4)	49 (11)	
		GCL	1.1 (1)	0	

The number of PCNA cells in different layers at 0 and 36 h of light treatment. Retinal sections were colabeled with PCNA and either GFAP, a Müller glial cell marker, or 4C4, a microglial cell marker. Three classes of PCNA-positive cells were observed at 0 h. All PCNA-positive cells located in the ONL, which were GFAP-negative and 4C4-negative, likely represent rod precursors. All PCNA-positive cells in the INL, which were also GFAP-positive, correspond to a very small percentage of Müller glial cells in the cell cycle in undamaged retinas. All PCNA-positive cells located in the GCL, which were 4C4-positive, likely represent microglial cells. At 36 h of light, 49% of the Müller glial cells reenter the cell cycle and are PCNA-positive. Numbers in the parentheses represent the standard error of the mean, ONL, outer nuclear layer; INL, inner nuclear layer; GCL, ganglion cell layer. All cell counts were obtained from a linear distance of 740 μm in the central dorsal retina.

Dev Neurobiol. Author manuscript; available in PMC 2013 July 15.

Table 2

Number of Different Nuclear Classes 28 Days After Light-Induced Damage

	Average Number of Nuclei Per Defined Linear Distance							
	GCL	*p*-Value	INL	*p*-Value	Müller Glia	*p-Value*	ONL	*p*-Value
Uninjected control	48 (5)	0.82	319 (15)	0.073	34 (1)	0.0001	161 (9)	0.0002
PCNA MO	50 (8)		281 (6)		16 (1)		52 (11)	

The number of nuclei in the ganglion cell layer (GCL), inner nuclear layer (INL), and outer nuclear layer (ONL) were quantified from frozen sections that were stained with TO-PRO-3, a nuclear stain. The number of Müller glial nuclei was quantified from glial fibrillary acidic protein (GFAP) immunolocalization on frozen sections. Both control and PCNA morphant retinas were treated in constant light for 4 days and returned to standard 14 h-light:10-h dark cycle for 28 days before analysis. Three sections (either containing the optic nerve or an adjacent section) from eight different eyes were quantified for each measurement. The number of nuclei was detemined per defined linear distance of 370 in the central dorsal retina. Numbers in parentheses represent the standard error of the mean. *p* values from statistical comparison across each group (GCL, INL, Muüller glia, and ONL) was determined by ANOVA.